Journal of Organometallic Chemistry 694 (2009) 2888–2897

Contents lists available at ScienceDirect

Journal of Organometallic Chemistry

journal homepage: www.elsevier.com/locate/jorganchem

Synthesis and electrochemical studies of η^5-monocyclopentadienylruthenium(II) complexes with substituted thiophene nitrile ligands. Crystal structure of $[Ru(\eta^5\text{-}C_5H_5)(dppe)(NC\{SC_4H_2\}_2NO_2)][PF_6]$

M. Helena Garcia [a,*], Paulo J. Mendes [b], M. Paula Robalo [c,d], M. Teresa Duarte [c], Nelson Lopes [e]

[a] Centro de Ciências Moleculares e Materiais, Faculdade de Ciências da Universidade de Lisboa, Ed.C8, Campo Grande, 1749-016 Lisboa, Portugal
[b] Centro de Química de Évora, Universidade de Évora, Rua Romão Ramalho 59, 7002-554 Évora, Portugal
[c] Centro de Química Estrutural, Instituto Superior Técnico, Universidade Técnica de Lisboa, Av. Rovisco Pais, 1049-001 Lisboa, Portugal
[d] Departamento de Engenharia Química, Instituto Superior de Engenharia de Lisboa, Rua Conselheiro Emídio Navarro, 1, 1959-007 Lisboa, Portugal
[e] Grupo de Lasers e Plasmas, Instituto de Plasmas e Fusão Nuclear, Instituto Superior Técnico, Universidade Técnica de Lisboa, Av. Rovisco Pais, 1049-001 Lisboa, Portugal

ARTICLE INFO

Article history:
Received 13 February 2009
Received in revised form 17 April 2009
Accepted 20 April 2009
Available online 3 May 2009

Keywords:
Ruthenium(II)
Monocyclopentadienyl
Thiophene ligands
Cyclic voltammetry
Second harmonic generation

ABSTRACT

A systematic series of η^5-monocyclopentadienylruthenium(II) complexes with substituted thiophene nitrile ligands of general formula $[Ru(\eta^5\text{-}C_5H_5)(P\_P)(NC\{SC_4H_2\}_nNO_2)][PF_6]$ (P_P = dppe, (+)-diop; n = 1–3) has been synthesized and characterized. Spectroscopic and electrochemical data were used in order to get an insight on the molecular nonlinear optical properties of these complexes when compared to those found for the reported thiophene iron(II) and *p*-benzonitrile or 1,2-di-(2-thienyl)-ethene derived iron(II)/ruthenium(II) related complexes. The compound $[Ru(\eta^5\text{-}C_5H_5)(dppe)(NC\{SC_4H_2\}_2NO_2)][PF_6]$ was also characterized by X-ray diffraction. The solid state nonlinear optical properties of the chiral compounds were also evaluated by Kurtz powder technique with a Nd:YAG laser emitting at 1064 nm.

1. Introduction

The exploitation of organometallic chemistry for the synthesis of new compounds with nonlinear optical (NLO) properties has been mainly motivated by the optical devices technology [1]. The significant work already published in this area during the last two decades [2–11] is in agreement with the general understanding that second-order nonlinearities are strongly related to asymmetric push–pull systems, both in organic and organometallic molecular materials. In the case of metallo-organic compounds, the metal centre can be bound to a highly polarizable conjugated backbone, acting hence as an electron releasing or withdrawing group. Consequently, strong charge-transfer (CT) transitions can occur, leading to high molecular first hyperpolarizabilities (β). Moreover, the position of these CT bands, usually appearing at the visible region, can be tuned by variation of the coligands and/or the metal itself, to optimize the hyperpolarizability through (near) resonant enhancement. This is the case of the general family of η^5-monocyclopentadienyliron(II)/ruthenium(II) complexes presenting benzene- or thiophene-based conjugated ligands coordinated to the metal centre through nitrile or acetylide linkages [12–16], which revealed to be much more efficient donor groups for second-order NLO purposes than the traditional organic donor groups (NMe_2, NH_2, etc.), leading therefore to higher β values.

Recently we found significant values of quadratic hyperpolarizabilities in complexes combining the organometallic donor fragment {FeCp(P_P)} (P_P = dppe, (+)-diop) with conjugated thiophene derived ligands. Measurements by hyper-Rayleigh scattering (HRS), in $[FeCp(dppe)(NC\{SC_4H_2\}_nNO_2)][PF_6]$ compounds with 1, 2 or 3 thiophene units presented values of β of 455, 710 and 910×10^{-30} esu, respectively, measured at 1064 nm [16]. Nevertheless, high values of β do not lead necessarily to good NLO efficiencies at the macroscopic level since the second-order NLO effects are strongly influenced by the crystal packing. Thus, crystallization in a non-centrosymmetric space group is a necessary criterion (not absolute) when solid state properties are evaluated, this being guaranteed in the present compounds by the chiral coligand, (+)-diop.

In order to get some hint about the solid state second harmonic generation efficiencies of the general family of compounds $[FeCp(P\_P)(NC\{SC_4H_2\}_nNO_2)][PF_6]$ we had extended our studies to the analogous family of ruthenium derivatives, which have the advantage of a higher transparency than the iron ones, at the second harmonic wavelength (532 nm) of the used Nd:YAG laser. These studies on bulk materials become very important when solid

* Corresponding author.
E-mail addresses: lena.garcia@fc.ul.pt, i017@alfa.ist.utl.pt (M.H. Garcia).

0022-328X/$ - see front matter © 2009 Elsevier B.V. All rights reserved.
doi:10.1016/j.jorganchem.2009.04.025

state applications are envisaged. The present paper reports the synthesis, characterization and electrochemical studies of a systematic series of η^5-monocyclopentadienylruthenium(II) complexes with nitro-substituted thiophene nitrile ligands of general formula $[RuCp(P\_P)(NC\{SC_4H_2\}_nNO_2)][PF_6]$ (P_P = dppe, (+)-diop; n = 1–3). The chiral (+)-diop coligand, as mentioned above, is used to favour the formation of a non-centrosymmetrical crystal structures, required for macroscopic second-order NLO. Spectroscopic and cyclic voltammetric data are compared with the values reported for other related η^5-monocyclopentadienyliron/ruthenium complexes and are evaluated at the light of the possible known electronic factors, responsible for the NLO properties. Preliminary evaluation of the efficiency on doubling frequency of a Nd:YAG laser emitting at 1064 nm was carried out for the ruthenium compounds possessing (+)-diop as coligand, $[RuCp((+)\text{-diop})(NC\{SC_4H_2\}_nNO_2)][PF_6]$ and one of the iron analogous, namely $[FeCp((+)\text{-diop})(NC\{SC_4H_2\}_2NO_2)][PF_6]$ by Kurtz powder technique.

2. Results and discussion

2.1. Synthesis and spectroscopic studies

The complexes (Fig. 1) were prepared by chloride abstraction of [RuCp(P_P)Cl] (P_P = dppe or (+)-diop) (dppe: 1,2-bis(diphenylphosphino)ethane; (+)-diop: (+)-2,3-*O*-isopropylidene-2,3-dihydroxy-1,4-bis(diphenylphosphino)butane) with $TlPF_6$ in the presence of an excess of the appropriate thiophene ligand in methanol or methanol/dichloromethane mixture, according to the solubility of the reactants, at room temperature. After workup, orange-reddish microcrystalline products of $[RuCp(P\_P)(NC\{SC_4H_2\}_nNO_2)][PF_6]$ (P_P = dppe, n = 1 (**1a**), n = 2 (**2a**), n = 3 (**3a**); P_P = (+)-diop, n = 1 (**1b**), n = 2 (**2b**), n = 3 (**3b**)) were obtained with yields in the range of 40–78%. The new compounds are fairly stable towards oxidation in air and to moisture both in the solid state and in solution. Formulation of the new compounds was supported by analytical data, IR and ^1H, ^{13}C and ^{31}P NMR spectroscopies. The molar conductivities of ca. 10^{-3} M solutions of the complexes in nitromethane, placed in the range 82–89 Ω^{-1} cm^2 mol^{-1}, are consistent with the values reported for 1:1 type electrolytes [17].

Typical IR bands confirm the presence of the cyclopentadienyl ligand (ca. 3120–3040 cm^{-1}), the PF_6^- anion (840 and 550 cm^{-1}) and the coordinated nitrile (2205–2225 cm^{-1}) in all the complexes. Comparison of ν(N≡C) upon coordination of the thiophene ligands to ruthenium(II) centres reveals a negative shift of −5 to −20 cm^{-1} for **1a**, **1b** and **2b** and a positive shift of +5 to +25 cm^{-1} for the remaining complexes (IR data of the nitrile ligands are from Ref. [16]). The negative shifts have been related with enhanced π-backdonation from the metal *d* orbitals to the π^* orbital of the NC group, which leads to a decrease in the N≡C bond order. In the present study the observed values show that the thiophene chain lengthening leads to a less effective π-backdonation interaction. Comparison of these shifts with those found on related thiophene iron(II) [16] and 1,2-di-(2-thienyl)-ethene iron(II) and ruthenium(II) [18] complexes leads to the following trend:

Fe-(thio)-NO_2 > Fe-(thio)-C(H)=C(H)-(thio)-NO_2 ≈ Fe-$(thio)_2$-NO_2 > Ru-(thio)-NO_2 > Ru-(thio)-C(H)=C(H)-(thio)-NO_2 ≈ Ru-$(thio)_2$-NO_2 > Fe-$(thio)_3$-NO_2 > Ru-$(thio)_3$-NO_2.

The magnitude of π-backdonation interaction is higher for iron(II) compounds as expected considering the better π-donor ability of the iron(II) moiety. Moreover in both iron(II) and ruthenium(II) families no significant differences are observed between the bithiophene derivatives and the ones possessing the vinylidene unit between the two thiophene rings. This behavior can ultimately give some insight on the trend of the corresponding first hyperpolarizabilities [16,19].

^1H NMR resonances for the cyclopentadienyl ring are in the range usually observed for monocationic ruthenium(II) complexes and depends mainly of the phosphine coligand being more shielded for (+)-diop complexes. The phosphine ^1H NMR resonances are also relatively insensitive to the nature of the aromatic nitrile. Considering the thiophene ligand protons, an overall shielding effect upon coordination was observed, especially for the H3 protons (see Table 1 and Fig. 2 for numbering scheme), indicating an electronic flow towards the aromatic ligand due to π-backdonation involving the metal centre. The same overall behavior on the ^1H NMR resonances was found in the similar iron(II) derivatives [16] and the 1,2-di-(2-thienyl)-ethene iron(II) and ruthenium(II) related compounds [18].

^{13}C NMR data generally confirm the evidences found in proton spectra and show the same behavior presented in the related iron(II) compounds [16]. The Cp ring resonances are in the range usually observed for monocationic ruthenium(II) complexes and depends mainly on the phosphine coligand as observed in ^1H NMR spectra. Also, the phosphine signals are relatively insensitive to the nature of the aromatic thiophene ligands. Considering the thiophene ligands, an expected deshielding on the NC carbon upon coordination was observed, whereas for the ring carbons more significant changes were observed for the carbons closest to the nitrile group (see Table 2), in agreement with the trends observed in the ^1H NMR spectra.

^{31}P NMR data for the complexes showed one singlet for dppe whereas for the (+)-diop coligand the resonances are characterized by two doublets, revealing the presence of two inequivalent phosphorous atoms.

The optical absorption spectra of all complexes were recorded using 5.0×10^{-5} M solutions in dichloromethane and DMF in order to identify metal-to-ligand and intraligand charge transfer bands (MLCT and ILCT, respectively), expected for these complexes. The spectra for **1a**–**3a** in dichloromethane typify the behavior of the compounds studied in this work (Fig. 3) and the optical data are

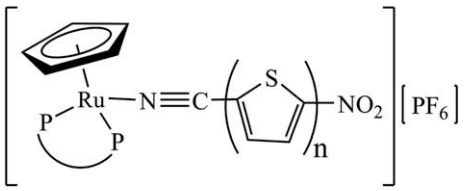

P_P=dppe: n=1 (**1a**), n=2 (**2a**), n=3 (**3a**)
P_P=(+)-diop: n=1 (**1b**), n=2 (**2b**), n=3 (**3b**)

Fig. 1. Structural formulae of the complexes $[RuCp(P\_P)(NC\{SC_4H_2\}_nNO_2)][PF_6]$.

Table 1
Differences on NMR ^1H resonances of thiophene ligands upon coordination to the Ru(II) organometallic fragments.[a,b]

Compound	$\Delta\delta^c$ (ppm)					
	H3	H4	H7	H8	H11	H12
1a	−0.59	−0.30	–	–	–	–
1b	−0.17	−0.11	–	–	–	–
2a	−0.85	−0.26	−0.09	−0.06	–	–
2b	−0.30	−0.01	−0.02	−0.03	–	–
3a	−0.68	−0.60	−0.10	−0.03	0.00	−0.02
3b	−0.31	−0.03	−0.03	0.00	0.01	0.00

[a] In $CDCl_3$ except **3a** and **3b** (in CD_2Cl_2).
[b] For ^1H NMR resonances of thiophene ligands see Ref. [16].
[c] $\delta_{complex} - \delta_{free\ ligand}$.

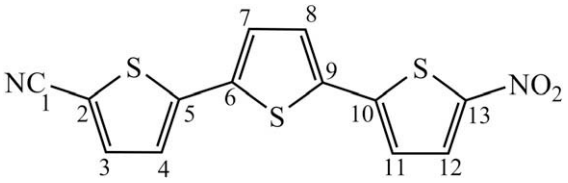

Fig. 2. Numbering scheme for NMR spectral assignments of Ru complexes and free ligands.

summarized in Table 3. The spectra of all compounds are characterized by the presence of absorption bands which assignment was based on the spectra of the free ligands and the organometallic fragments $[RuCp(P\_P)]^+$. The electronic transition of the organometallic moiety ($\lambda \sim 253$–265 nm) and of the uncoordinated thiophene ligands ($\lambda \sim 289$–442 nm) can be clearly recognized in the spectra of all the complexes. An important feature for the compounds **1a** and **1b** is the appearance of two new weak broad bands in the visible region ($\lambda \sim 388$–485 nm) assigned to MLCT

Table 2
Differences on NMR ^{13}C resonances of thiophene ligands upon coordination to the Ru(II) organometallic fragments.[a,b]

Compound	$\Delta\delta$[c] (ppm)												
	C1	C2	C3	C4	C5	C6	C7	C8	C9	C10	C11	C12	C13
1a	3.12	1.91	2.25	0.50	−1.11	–	–	–	–	–	–	–	–
1b	5.81	1.85	3.24	0.97	−0.60	–	–	–	–	–	–	–	–
2a	7.17	−1.15	2.00	0.38	−0.16	0.32	0.46	−1.21	−0.24	–	–	–	–
2b	9.60	−2.05	2.60	0.91	0.63	−0.12	0.70	−0.65	−0.05	–	–	–	–
3a	6.92	−1.91	1.05	0.61	1.00	−0.44	−0.21	0.22	0.41	−0.22	−0.10	0.04	−0.02
3b	10.76	−2.25	1.67	0.69	1.96	−0.24	0.43	0.34	0.32	−0.26	0.23	0.27	0.20

[a] In $CDCl_3$ except **3a** and **3b** (in CD_2Cl_2).
[b] For ^{13}C NMR resonances of thiophene ligands see Ref. [16].
[c] $\delta_{complex} - \delta_{free\ ligand}$.

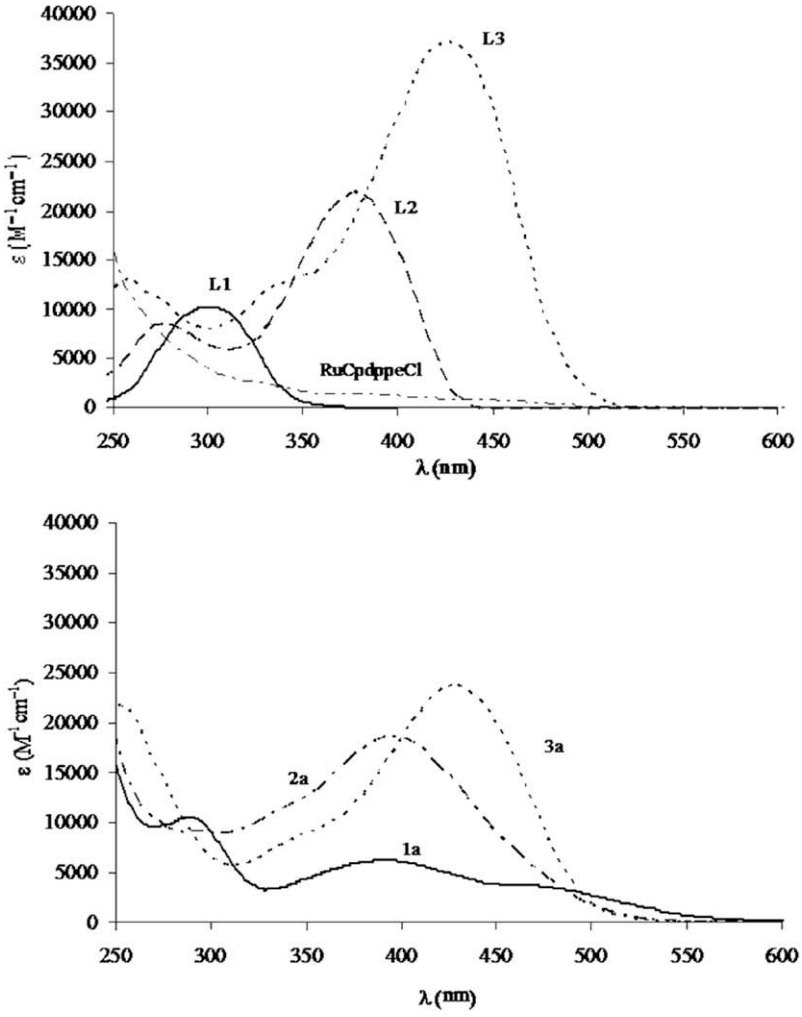

Fig. 3. Absorption spectra of $[RuCp(dppe)(NC\{SC_4H_2\}_nNO_2)][PF_6]$ ($n = 1$: **1a**, $n = 2$: **2a**, $n = 3$: **3a**) recorded in CH_2Cl_2 (5.0×10^{-5} M). Top figure shows absorption spectra for the free thiophene ligands $NC\{SC_4H_2\}_nNO_2$ ($n = 1$: **L1**, $n = 2$: **L2**, $n = 3$: **L3**) taken from Ref. [16] and RuCp(dppe)Cl in the same experimental conditions for comparison.

Table 3
Selected electronic spectral data for $[RuCp(P\_P)(NC\{SC_4H_2\}_nNO_2)][PF_6]$ complexes in dichloromethane solution (ca. 5.0×10^{-5} M).

Compound	λ, nm (10^{-4} ε)
1a	253 (sh), 289 (0.97), 389 (0.58), 485 (0.24)
1b	265 (sh), 292 (sh), 388 (0.66), 471 (0.38)
2a	254 (sh), 329 (sh), 396 (1.62), 452 (0.51)
2b	264 (sh), 322 (sh), 395 (2.02), 442 (0.33)
3a	257 (sh), 429 (2.39)
3b	262 (sh), 442 (1.97)

transitions. For the compounds with two and three thiophene rings, these MLCT transitions are more difficult to assign due to the possible overlapping with the ILCT transition associated to the thiophene chromophores.

In order to clarify this hypothesis a fit with multiple GAUSSIANS bands were applied to the spectra of these compounds, which reveal longest wavelength absorption bands at 452 nm (**2a**) and 442 nm (**2b**) that are compatible with MLCT transitions. However, these bands were not clearly found for **3a** and **3b** due to the complete overlapping with ILCT transition related to the ligand **L3**. In fact, the MLCT transitions seems to shift to higher energies with increasing conjugation length while the intraligand bands shift to lower energies, this giving a complete overlapping of these bands for the compounds with three thiophene rings. The same behavior was already found in the similar iron(II) complexes [16]. Compared to these iron(II) complexes, the MLCT bands on the ruthenium(II) derivatives are shifted to higher energies. According to the well known two-level-model (TLM) [20] this behavior can ultimately lead to lower quadratic hyperpolarizabilities for the ruthenium(II) complexes. On the basis of this model, it might be expected similar quadratic hyperpolarizabilities for **2a** and for the thiophen-2-yl-vinyl-thiophene ruthenium(II) derivative [18] since no significant differences on the energies of the corresponding lowest-energy bands were found.

The most relevant results concerning the solvatochromic behavior of all compounds are summarized in Table 4. Although these results must be carefully analyzed due to the broadening of the bands, which lead to some uncertainty in the attribution of λ_{max} values, the studies showed a slight bathochromic shift on the MLCT bands for the compounds **1a** and **1b** upon increasing the polarity of the solvent. This positive solvatochromic behavior is characteristic of electronic transitions with an increase of the dipole moment upon photo-excitation.

2.2. Electrochemical studies

In order to get an insight on the electron richness of the organometallic fragment and the coordinated chromophores, the electrochemical behavior of Ru(II) complexes was studied by cyclic voltammetry in dichloromethane and acetonitrile, between the limits imposed by the solvents. The cyclic voltammetry of the free thiophene ligands was reported elsewhere [16]. As an example, the electrochemical response for **2a** in dichloromethane is shown in Fig. 4, and the most relevant data for redox changes exhibited by all the complexes in dichloromethane and acetonitrile are summarized in Tables 5 and 6.

The electrochemical behavior in dichloromethane is characterized by the presence of one quasi-reversible redox process attributed to Ru(II)/Ru(III) couple, in the range 1.17–1.41 V, and two reductive processes occurring on the coordinated nitrile ligands. In addition, low intense redox waves at $E_{p/2} \approx 0.12$ V and $E_{pa} \approx -0.95$ V were found and attributed to decomposition products originated by the second reductive process since these waves vanish when the potential is reverted immediately after the first reductive process (Fig. 4). A difference of 60–100 mV on Ru(II)/Ru(III) couple was found from **1** to **2** compounds, whereas between **2** and **3** the difference is only 10–30 mV. This behavior is analogous to the one observed for similar iron(II) complexes [16] and can be explained by a less effective release of electronic density from the metal centre to the acceptor nitro group with the extension of the aromatic system. These results confirm the evidences of the spectroscopic data discussed above, namely the relative magnitude of the metal-ligand π-backdonation, which was found to decrease as the conjugation length of the nitrile ligand increases. Replacing dppe coligand by (+)-diop gives an expected increase of the redox potential of the Ru(II)/Ru(III) couple, which agrees with the relative donating ability of the two organometallic fragments. As the HOMO energy can be related to the Ru(II)/Ru(III) potential [16,21] the results discussed above show that this orbital, as expected, is destabilized by dppe and, in a less extent, by the chain lengthening of the thiophene ligand. These overall results are illustrated in Fig. 5, in which electrochemical data for similar iron(II) complexes were also added for comparison.

As mentioned above, all complexes show two redox processes at negative potentials, occurring at the coordinated thiophene ligands. The first redox couple, in the range −0.56 V to −0.86 V, is reversible or quasi-reversible and corresponds to the formation of the anionic radical. The results show that LUMO, which energy can be related to this first reduction potential [16,21], is destabilized as the chain-length of the thiophene ligand increases and is

Table 4
Relevant solvatochromic data for $[RuCp(P\_P)(NC\{SC_4H_2\}_nNO_2)][PF_6]$ complexes.

Compound	λ (nm)	
	CH_2Cl_2	DMF
1a	389	408
	485	504
1b	388	419
	471	485
2a	396	418
	452	481
2b	395	407
	442	474
3a	428	454
3b	442	445

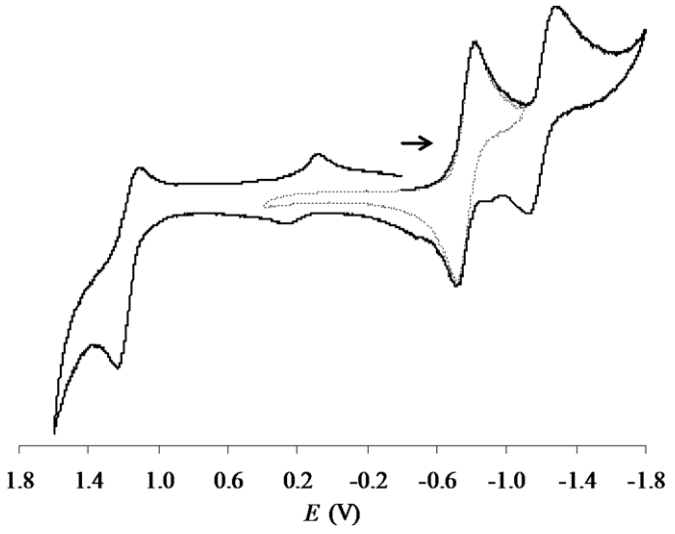

Fig. 4. Cyclic voltammograms of **2a** in dichloromethane showing both oxidative and reductive processes (—) and the first reductive process (- - -) at scan rate of 200 mV/s.

Table 5
Electrochemical data for [RuCp(P_P)(NC{SC_4H_2}$_n$$NO_2$)][$PF_6$] complexes in CH_2Cl_2.

Compound	E_{pc} (V)	E_{pa} (V)	$E_{p/2}$ (V)	$E_{pa} - E_{pc}$ (mV)	I_c/I_a
1a	1.23	1.33	1.28	100	0.6
	−0.65	−0.56	−0.61	90	1
	−1.35	–	–	–	–
1b	1.35	1.47	1.41	120	0.8
	−0.61	−0.5	−0.56	110	1
	−1.23	−1.1	–	–	–
2a	1.12	1.23	1.18	110	0.7
	−0.82	−0.72	−0.77	100	1
	−1.27	−1.15	−1.21	120	1
2b	1.29	1.4	1.35	110	0.7
	−0.8	−0.71	−0.76	90	1
	−1.21	−1.12	−1.17	90	1
3a	1.11	1.22	1.17	110	0.8
	−0.91	−0.81	−0.86	100	1
	−1.24	−1.15	−1.19	90	0.6
3b	1.26	1.37	1.32	110	0.6
	−0.93	−0.82	−0.88	110	0.8
	−1.23	−1.15	−1.19	80	0.6

Table 6
Electrochemical data for [RuCp(P_P)(NC{SC_4H_2}$_n$$NO_2$)][$PF_6$] complexes in acetonitrile.

Compound	E_{pc} (V)	E_{pa} (V)	$E_{p/2}$ (V)	$E_{pa} - E_{pc}$ (mV)	I_c/I_a
1a	–	1.16	–	–	–
	1.00[a]	–	–	–	–
	−0.62	−0.56	−0.6	60	1
	−1.27	−1.2	−1.24	70	1
1b	–	1.35	–	–	–
	1.16[b]	–	–	–	–
	−0.58	−0.5	−0.54	80	0.9
	−1.3	−1.01	–	–	–
2a	–	1.09	–	–	–
	1.00[a]	–	–	–	–
	−0.79	−0.72	−0.76	70	1
	−1.22	−1.15	−1.18	70	1
2b	–	1.29	–	–	–
	1.16[b]	–	–	–	–
	−0.78	−0.69	−0.74	90	0.9
	−1.19	−1.1	−1.15	90	0.9
3a	–	1.54	–	–	–
	–	1.08	–	–	–
	1.00[a]	–	–	–	–
	−0.87	−0.81	−0.84	60	1
	−1.24	−1.18	−1.21	60	0.9
3b	–	1.6	–	–	–
	–	1.27	–	–	–
	1.16[b]	–	–	–	–
	−0.86	−0.79	−0.83	70	0.7
	−1.23	−1.15	−1.19	80	0.8

[a,b] Waves assigned to reduction of $[RuIIICp(P_P)(NCMe)]^{2+}$ (see text).

only slightly affected by the nature of the phosphine coligand. The second reduction is reversible or quasi-reversible for the compounds **2** and **3** whereas for compounds with one thiophene ring one fully irreversible wave was found. On the basis of HOMO–LUMO gap, as expressed by the difference between the $E_{p/2}$ for the oxidation process and the $E_{p/2}$ for the first reduction process, the results show that this gap depends on the phosphine coligand and the chain lengthening of the thiophene ligand (Table 7). As expected, the lower HOMO–LUMO gaps observed for dppe complexes are mainly due to the higher energies of the HOMOs since LUMOs, mainly located on thiophene ligands, are only slightly affected by the nature of the phosphine coligand. The chain lengthening of the thiophene ligands lead to an increase of the HOMO–LUMO gap, mainly as a result of the destabilizing effect

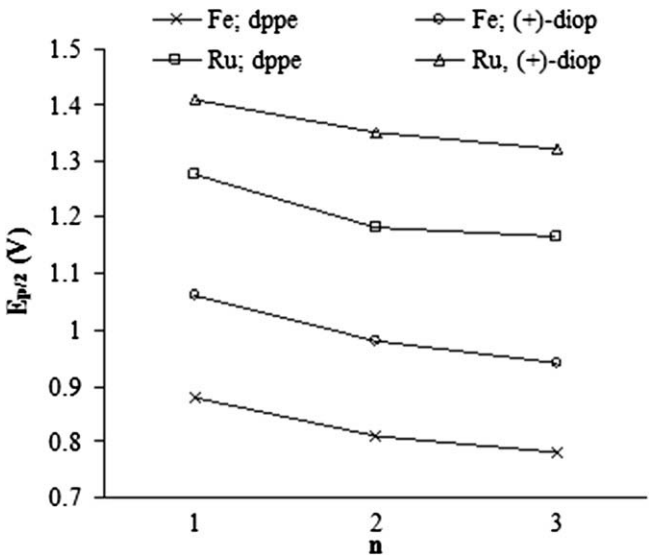

Fig. 5. Trends on oxidation potentials, in CH_2Cl_2, for Ru(II) and Fe(II) [MCp(P_P)(NC{SC_4H_2}$_n$$NO_2$)][$PF_6$] complexes. Iron data collected from Ref. [16].

Table 7
Estimation of HOMO–LUMO gaps based on electrochemical data in CH_2Cl_2 for [MCp(P_P)(NC{SC_4H_2}$_n$$NO_2$)][$PF_6$] complexes.

Compound	$E_{ox} - E_{red}$ (V)	
	Ru	Fe[a]
[MCp(dppe)(NC{SC_4H_2}NO_2)]+	1.89	1.50
$[MCp((+)\text{-diop})(NC\{SC_4H_2\}NO_2)]^+$	1.97	1.64
$[MCp(dppe)(NC\{SC_4H_2\}_2NO_2)]^+$	1.95	1.63
$[MCp((+)\text{-diop})(NC\{SC_4H_2\}_2NO_2)]^+$	2.11	1.76
$[MCp(dppe)(NC\{SC_4H_2\}_3NO_2)]^+$	2.03	1.69
$[MCp((+)\text{-diop})(NC\{SC_4H_2\}_3NO_2)]^+$	2.20	1.84

[a] Data taken from Ref. [16] for comparison.

on LUMO, as previously discussed and also recently reported in the study of the related thiophen-2-yl-vinyl-thiophene derivatives [18]. Similar trends were observed on similar iron(II) complexes [16] but higher HOMO–LUMO gaps are found for ruthenium(II) complexes. This is mainly due to the stabilization of the HOMO orbitals for the ruthenium(II) derivatives, since the LUMO energies are almost unaffected by changing the metal fragment. In fact, the oxidation potentials for ruthenium(II) compounds are *ca.* 0.38 V higher than the iron(II) ones, whereas the first reduction potentials are very similar for both metals, considering the same thiophene ligand [16]. These results are in agreement with the better donor character of the iron(II) fragment.

Our previous observation that thiophene ligands can be substituted by the acetonitrile solvent during the oxidative process in the electrochemical experiments [16], was also found for these ruthenium(II) compounds. In fact, our electrochemical studies in acetonitrile showed that the Ru(II)/Ru(III) oxidation have no cathodic counterpart for all the studied complexes. Moreover, a new cathodic wave arises at 1.00 V for the complexes with dppe and at 1.16 V for (+)-diop complexes independently of the coordinated thiophene ligand (see Table 6). These cathodic potentials were assigned to the reduction of the 17-electron species $[RuCp(P_P)(NCCH_3)]^{2+}$ since the values are consistent with those found in separate electrochemical experiments for the redox couple of $[RuCp(P_P)(NCCH_3)][PF_6]$ compounds. These results seem to indicate that the 17-electron species [RuCp(P_P)(NC{SC_4H_2}$_n$-NO_2)]$^{2+}$, formed on the electrode surface at the oxidation potential, undergo fast substitution of thiophene ligand by acetonitrile solvent molecule, leading to the $[RuCp(P_P)(NCCH_3)]^{2+}$ species.

The electrochemical experiments in acetonitrile showed the same general trend on the oxidation and reduction potentials by varying the phosphines co-ligands and the thiophene chromophores that was observed in dichloromethane.

2.3. X-ray structural studies

Crystals of [RuCp(dppe)(NC{SC_4H_2}$_2NO_2$)][PF_6] were obtained by slow diffusion of *n*-hexane in a dichloromethane solution at room temperature. The molecular structure of **2a** (Fig. 6 and Table 8 for selected bond distances and angles) was established by X-ray diffraction analysis. The overall geometry around ruthenium can be described as pseudo-octahedral, on the assumption that the cyclopentadienyl group takes up three coordination sites. The structural data derived from the geometry around the metal, namely the P1–Ru1–P2, N1–Ru1–P1 and N1–Ru1–Cp angles are similar to the other cyclopentadienyl complexes reported in the literature [22,23].

The bond lengths Ru–P and Ru–Cp and P1–Ru–P2 angle re similar to those found in the analogous complex [RuCp(dppe)(*p*-NC{C_6H_4}$_2NO_2$)][PF_6] [22] and are within the values found in the literature [23b,23d]. The Ru1–N1 distance, 2.005(5) Å, is slightly higher than the one found for [RuCp(dppe)(NC(C_4H_2S)C(H)C(H)(C_4H_2S)NO_2)][PF_6] and shorter than other ruthenium complexes containing nitriles (Table 9). The nitrile bond distance, very similar to the one observed for [RuCp(dppe)(NC(C_4H_2S)C(H)C(H)(C_4H_2S)-NO_2)][PF_6], although marginally shorter, is comparable with the other complexes and indicate a triple bond character. These results suggest some evidence for a slight poorer degree of π-backdonation for **2a** when compared to [RuCp(dppe)(NC(C_4H_2S)C(H)C(H)(C_4H_2S)NO_2)][PF_6], supported also by the spectroscopic data. The nitrile group shows an almost linear geometry with the C1–N1–Ru1 and N1–C1–C2 angles being 175.4(5)° and 177.0(7)°, respectively. The dihedral angle between the planes of the thiophene rings (17.6°) is higher than the corresponding one in the related compound [RuCp(dppe)(NC(C_4H_2S)C(H)C(H)(C_4H_2S)NO_2)][PF_6] (8.39°) [18], resulting in a somewhat lower planarity for the present compounds. The dihedral angle between the thiophene rings may in fact have some influence in the loss of charge transfer efficiency with increasing conjugated length, as suggested for the compounds [FeCp(dppe)(NC{C_4H_2S}$_n$$NO_2$)][$PF_6$] (*n* = 2, 3) [16]. Distances and angles within the thiophene rings are consistent with the retention of aromaticity, in particular there is no obvious bond length alternation which would be expected for an appreciable quinoidal contribution.

The crystal packing of **2a** is centrosymmetric due to the crystallization in the monoclinic space group $P2_1/n$ with four independent molecules in the unit cell, making this compound unsuitable for solid state NLO purposes. However multiple intermolecular hydrogen bonding motif in the solid state are observed involving the PF_6^- counterion and several hydrogens of the cationic counterpart.

2.4. Second-order NLO characterization

The nonlinear optical properties, namely the second harmonic generation (SHG), of compounds [RuCp((+)-diop)(NC{SC_4H_2}$_n$-

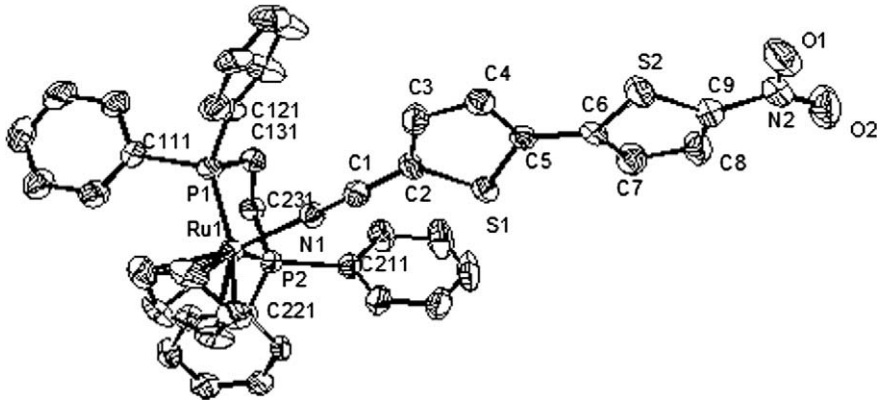

Fig. 6. Molecular structure of the [RuCp(dppe)(NC{SC_4H_2}$_2NO_2$)]$^+$, showing the labelling scheme. Hydrogen atoms have been omitted for clarity.

Table 8
Selected bond lengths (Å) and angles (°) for [RuCp(dppe)(NC{SC_4H_2}$_2NO_2$)][PF_6] (**2a**).

Bond lengths (Å)				Angles (°)			
Ru1–N1	2.005(5)	N1–C1	1.143(6)	N1–Ru1–C21	154.3(2)	C211–P2–Ru1	112.7(2)
Ru1–Cp[a]	1.8637	C1–C2	1.407(7)	C21–Ru1–P1	118.2(2)	C221–P2–Ru1	118.7(2)
Ru1–C21	2.186(6)	C2–C3	1.358(8)	C21–Ru1–P2	101.7(2)	C131–P1–Ru1	108.7(2)
Ru1–P1	2.293(1)	C3–C4	1.394(8)	N1–Ru1–Cp[a]	122.7	C231–P2–Ru1	109.5(2)
Ru1–P2	2.286(1)	C4–C5	1.363(8)	N1–Ru1–P1	85.0(1)	C231–C131–P1	107.4(4)
C21–C22	1.379(9)	C2–S1	1.726(6)	N1–Ru1–P2	91.1(1)	C131–C231–P2	109.6(4)
C22–C23	1.411(9)	C5–S1	1.719(5)	P1–Ru1–P2	83.92(5)	C1–N1–Ru1	175.4(5)
C23–C24	1.392 (9)	C5–C6	1.443(7)	Ru1–P1–Cp[a]	133.4	N1–C1–C2	177.0(7)
C24–C25	1.40(1)	C6–C7	1.355(8)	Ru1–P2–Cp[a]	126.9	C9–N2–O1	119.1(6)
C25–C21	1.402(9)	C7–C8	1.398(8)	C111–P1–Ru1	120.6(2)	C9–N2–O2	114.3(6)
P1–C111	1.827(6)	C8–C9	1.330(9)	C121–P1–Ru1	114.8(2)		
P1–C121	1.827(6)	C6–S2	1.722(5)				
P1–C131	1.857(5)	C9–S2	1.692(6)				
P2–C211	1.823(6)	C9–N2	1.458(8)				
P2–C221	1.834(6)	N2–O1	1.187(7)				
P2–C231	1.841(6)	N2–O2	1.235(7)				

[a] Cp centroid.

Table 9
Structural data for monocyclopentadienylruthenium(II) derivatives with nitrile ligands.

Compound	Bond lengths (Å)			Angles (°)		Ref.
	Ru–N1	N1–C1	C1–C2	Ru–N1–C1	N1–C1–C2	
$[RuCp(dppe)(NC\{SC_4H_2\}_2NO_2)][PF_6]$	2.005(5)	1.144(6)	1.407(7)	175.4(5)	177.1(7)	This work
$[RuCp(dppe)(NC(C_4H_2S)C(H)C(H)(C_4H_2S)NO_2)][PF_6]$	1.997(5)	1.148(8)	1.436(10)	175.8(5)	176.4(7)	[18]
$[RuCp(dppe)(p\text{-}NC(C_6H_4)_2NO_2)][PF_6]$	2.021	1.126	1.46	175.8	176.1(12)	[22]
$[RuCl_2(CO)_2(NCC_6H_5)_2]$	2.119(2)	1.138(8)	1.439(9)	175.5(1)	177.1(20)	[24a]
$[RuCp(PPh_3)_2(p\text{-}NC(C_6H_4)_2OEt)][PF_6]$	2.041(5)	–	–	–	–	[24b]
$[RuCl_4(NCC_6H_5)_2][Bu_4N]$	2.024 2.002	1.124 1.135	1.447	176.3	–	[25]

$NO_2)][PF_6]$ ($n = 1$–3) and $[FeCp((+)\text{-diop})(NC\{SC_4H_2\}_2NO_2)][PF_6]$ [16] were evaluated with our experimental set up [26], for measurements by the Kurtz powder technique [27]. The studies were performed at the Nd:YAG laser fundamental wavelength (1064 nm) considering the reasonable transparence of the samples at 532 nm, the second harmonic wavelength. The efficiency in doubling the laser frequency was only detectable for the $[RuCp((+)\text{-diop})(NC\{SC_4H_2\}NO_2)][PF_6]$ (**1b**) complex, which emitted a signal approximately 100 times smaller than the standard urea. For the other studied compounds the emitted signals were negligible. It is important to become aware that the results obtained by this technique are very difficult to interpret in terms of molecular structure-property relationships, since they depend not only on the molecular hyperpolarizability β but also very strongly of the solid state effects, such as for example, the crystal packing structure, grain size and the phase matching properties. To better understand the results of the present study, it would be crucial to consider the X-ray data relative to the precise orientation of the molecules in the crystal and, even more important, the angle between the molecular charge transfer axis (typically along the donor–acceptor axis) and the polar crystal axis. It is known that there is an optimum value for this angle which depends of the crystal space group in order to allow quadratic phase-matched interactions [28–30]. Thus, the poor values found for these compounds can be probably explained by a significant deviation from the optimal phase matching direction. Finally, it is important to point out that these preliminary studies did not account for fluorescence and grain size of the samples. Some work is in progress to obtain crystals suitable for X-ray studies.

3. Conclusions

A new family of Ru(II) half-sandwich complexes was synthesised and fully characterized. As already found for the previously reported related thiophene iron(II) complexes, spectroscopic and electrochemical data suggest an improved electronic π-coupling between the η^5-cyclopentadienylruthenium(II) moiety and the π-system of the conjugated thiophene ligands, when compared to the previously reported *p*-benzonitrile analogues. However, a poorer electron-donor effect from the metal centre towards NO_2 acceptor group is found for the complexes studied in this work. Also, spectroscopic, electrochemical and crystallographic data show marginally differences between the $[RuCp(dppe)(NC\{C_4H_2S\}_2NO_2)][PF_6]$ and the related $[RuCp(dppe)(NC(C_4H_2S)C(H)=C(H)(C_4H_2S)NO_2)][PF_6]$ complex, despite some improved electronic coupling between the organometallic fragment and the nitrile ligand for the thiophene-vinyl derivative. Thus, the overall data suggest an expected improvement of the quadratic hyperpolarisabilities for the complexes studied in the present work when compared to those found in *p*-benzonitrile derivatives. Nevertheless these values are expected lower than the similar thiophene iron(II) complexes. Despite some poorer electronic coupling between the ruthenium(II) fragment and the nitrile ligand for the bithiophene derivative when compared to that found in related thiophen-2-yl-vinyl-thiophene reported in the literature, we expected comparable quadratic hyperpolarizabilities for these complexes. Finally, in spite of the somewhat lower β values expected for the (+)-diop complexes, the SHG efficiencies found by Kurtz powder technique, in the preliminary tests carried out in the present study, were unsatisfactory and can probably find some justification in the multiple factors related with the used method.

4. Experimental

4.1. General procedures

All preparations and manipulations of the complexes described in this work were carried out under nitrogen or argon atmosphere using standard Schlenck techniques. Solvents were purified according to the usual methods [31]. Solid state IR spectra were taken on a Perkin–Elmer 457 spectrophotometer with KBr pellets; only significant bands are cited in the text. ^1H, ^{13}C and ^{31}P NMR spectra were recorded on a Varian Unity 300 spectrometer at probe temperature. The ^1H and ^{13}C chemical shifts are reported in parts per million (ppm) downfield from internal Me_4Si and the ^{31}P NMR spectra are reported in ppm downfield from external standard 85% H_3PO_4. Coupling constants are reported in Hz. Spectral assignments follow the numbering scheme shown in Fig. 2. Electronic spectra were recorded at room temperature on a Shimadzu UV-1202 spectrometer. Melting points were obtained using a Reichert Thermovar. The molar conductivities of 1 mM solutions of the complexes in nitromethane were recorded with a Schott CGB55 Konduktometer at room temperature. Microanalyses were obtained at the Laboratório de Análises, Instituto Superior Técnico, using a Fisons Instruments EA1108 system. Data acquisition, integration and handling were performed using a PC with the software package Eager-200 (Carbo Erba Instruments).

The starting ruthenium(II) complexes [RuCp(dppe)Cl], [RuCp((+)-diop)Cl] [32] and thiophene ligands 5-nitrothiophene-2-carbonitrile (**L1**), 5′-nitro-2,2′-bithiophene-5-carbonitrile (**L2**) and 5″-nitro-2,2′:5′,2″-terthiophene-5-carbonitrile (**L3**) [16] were prepared as reported.

4.2. Synthesis of the complexes

All the complexes $[RuCp(P\_P)(NC\{SC_4H_2\}_nNO_2)][PF_6]$ (P_P = dppe or (+)-diop; $n = 1$, 2 or 3) were prepared as follows: $TlPF_6$ (0.37 mmol) was added to a solution of [RuCp(P_P)Cl] (0.33 mmol) and the appropriate thiophene derivative (0.39 mmol) in methanol or a mixture of methanol/dichloromethane according to the solubility of the reactants. The suspension was stirred at room temperature for 16–96 h. A change was observed from yellow-orange to orange-reddish with simultaneous precipitation of TlCl and some desired product. After filtration, the solvent was evaporated under vacuum and the solid residue washed several times with diethyl ether/dichloromethane mixture to remove the

excess of thiophene ligand derivative. Furthermore, the desired product co-precipitated with TlCl was solubilized with dichloromethane and filtered to remove the thallium salt. The solvent was evaporated under vacuum and the solid obtained was recrystallized together with previous isolated residue from dichloromethane/*n*-hexane or dichloromethane/diethyl ether giving the desired complexes as orange-reddish microcrystalline products.

^{1}H and ^{13}C NMR data relative to dppe and (+)-diop coordinated phosphines are very similar in the ruthenium(II) compounds, and are described below.

*Compounds **1a** and **2a**. For dppe*: ^{1}H NMR ($CDCl_3$): 2.56–2.68 (m, 4H, CH_2), 7.22–7.29 (m, 4H, C_6H_5), 7.43–7.54 (m, 8H, C_6H_5), 7.58 (t, 4H, C_6H_5, $^3J_{HH}$ = 7.5), 7.78 (m, 4H, C_6H_5, $^3J_{HH}$ = 8.5); ^{13}C NMR ($CDCl_3$): δ 28.08 (t, CH_2, $^1J_{CP}$ = 23.0), 129.12 and 129.50 (t, C_{meta}, $^3J_{CP}$ = 4.8), 130.58 and 133.03 (t, C_{ortho}, $^2J_{CP}$ = 4.8), 130.64 and 131.27 (s, C_{para}), 136.98 (t, C_{ipso}, $^1J_{CP}$ = 2.8).

*Compound **3a**. For dppe*: ^{1}H NMR (CD_2Cl_2): δ 2.58–2.66 (m, 4H, CH_2), 7.26–7.32 (m, 4H, C_6H_5), 7.46–7.50 (m, 6H, C_6H_5), 7.57–7.62 (m, 6H, C_6H_5), 7.76–7.82 (m, 4H, C_6H_5); ^{13}C NMR (CD_2Cl_2): δ 28.23 (t, CH_2, $^1J_{CP}$ = 22.8), 129.41 and 129.66 (t, C_{meta}, $^3J_{CP}$ = 4.9), 130.98 and 131.55 (s, C_{para}), 131.09 and 133.36 (t, C_{ortho}, $^2J_{CP}$ = 4.8), 137.25 (t, C_{ipso}, $^1J_{CP}$ = 2.8).

*Compounds **1b** and **2b**. For (+)-diop*: ^{1}H NMR ($CDCl_3$): δ 1.14 (s, 3H, CH_3), 1.31 (s, 3H, CH_3), 2.31–2.41 (m, 1H, CH), 2.58–2.68 (m, 1H, CH), 3.10–3.31 (m, 2H, CH_2), 3.48–3.64 (m, 2H, CH_2), 7.11–7.18 (m, 4H, C_6H_5), 7.40–7.46 (m, 6H, C_6H_5), 7.54–7.60 (m, 4H, C_6H_5), 7.66–7.72 (m, 4H, C_6H_5), 7.85–7.92 (m, 2H, C_6H_5); ^{13}C NMR ($CDCl_3$): δ 26.73 (s, CH_3), 26.90 (s, CH_3), 29.04 (d, CH_2, $^1J_{CP}$ = 21.4), 30.75 (d, CH_2, $^1J_{CP}$ = 3.4), 75.58 (d, CH, $^2J_{CP}$ = 11.7), 78.36 (d, CH, $^2J_{CP}$ = 6.2), 109.06 (s, $C(CH_3)_2$), 128.82–134.34 (m, C_6H_5), 138.78 (d, C_{ipso}, $^1J_{CP}$ = 47.6), 141.06 (d, C_{ipso}, $^1J_{CP}$ = 46.4).

*Compound **3b**. For (+)-diop*: ^{1}H NMR (CD_2Cl_2): δ 1.06 (s, 3H, CH_3), 1.26 (s, 3H, CH_3), 2.32–2.43 (m, 1H, CH), 2.60–2.67 (m, 1H, CH), 3.15–3.25 (m, 2H, CH_2), 3.58–3.70 (m, 2H, CH_2), 7.38–7.48 (m, 10H, C_6H_5), 7.54–7.80 (m, 8H, C_6H_5), 7.85–7.91 (m, 2H, C_6H_5); ^{13}C NMR (CD_2Cl_2): δ 26.85 (s, CH_3), 26.98 (s, CH_3), 29.19 (d, CH_2, $^1J_{CP}$ = 21.0), 32.00 (d, CH_2, $^1J_{CP}$ = 29.0), 75.80 (d, CH, $^2J_{CP}$ = 11.6), 78.72 (d, CH, $^2J_{CP}$ = 9.4), 109.41 (s, $C(CH_3)_2$), 129.10–134.83 (m, C_6H_5), 138.93 (d, C_{ipso}, $^1J_{CP}$ = 41.8), 141.92 (d, C_{ipso}, $^1J_{CP}$ = 38.4).

4.2.1. [RuCp(dppe)(NC{SC_4H_2}NO_2)]PF_6 (**1a**)

78% yield, red, recrystallized from CH_2Cl_2/*n*-hexane, m.p. 224–226 °C. Molar conductivity (Ω^{-1} cm^2 mol^{-1}) 87.4. IR (KBr) cm^{-1}: υ (N≡C) 2220. ^{1}H NMR ($CDCl_3$): δ 4.87 (s, 5H, η^5-C_5H_5), 7.00 (d, 1H, H3, $^3J_{HH}$ = 4.5), 7.61 (d, 1H, H4, $^3J_{HH}$ = 4.5); ^{13}C NMR ($CDCl_3$): δ 83.27 (η^5-C_5H_5), 113.84 (C2), 118.55 (NC), 128.04 (C4), η 138.62 (C3), 154.51 (C5); ^{31}P NMR ($CDCl_3$): δ 79.3. Anal. Calc. for $C_{36}H_{31}F_6N_2O_2P_3SRu$: C, 50.06; H, 3.62, N, 3.24; S, 3.71. Found: C, 50.32; H, 3.65, N, 3.08; S, 3.42%.

4.2.2. RuCp(dppe)(NC{SC_4H_2}$_2NO_2$)]PF_6 (**2a**)

72% yield, orange; recrystallized from CH_2Cl_2/*n*-hexane, m.p. 255 °C (dec.). Molar conductivity (Ω^{-1} cm^2 mol^{-1}) 86.8. IR (KBr) cm^{-1}: υ (N≡C) 2225. ^{1}H NMR ($CDCl_3$): δ 4.85 (s, 5H, η^5-C_5H_5), 6.76 (d, 1H, H3, $^3J_{HH}$ = 4.2), 7.07 (d, 1H, H4, $^3J_{HH}$ = 4.2), 7.13 (d, 1H, H7, $^3J_{HH}$ = 4.2), 7.83 (d, 1H, H8, $^3J_{HH}$ = 4.2); ^{13}C NMR ($CDCl_3$): δ 82.74 (η^5-C_5H_5), 109.81 (C2), 120.37 (NC), 125.14 (C7), 126.44 (C4), 128.14 (C8), 140.37 (C3), 141.14 (C5), 141.71 (C6), 151.22 (C9); ^{31}P NMR ($CDCl_3$): δ 79.6. Anal. Calc. for $C_{40}H_{33}F_6N_2O_2P_3S_2Ru$: C, 50.80; H, 3.52, N, 2.96; S, 6.78. Found: C, 50.92; H, 3.64, N, 2.88; S, 6.51%.

4.2.3. RuCp(dppe)(NC{SC_4H_2}$_3NO_2$)]PF_6 (**3a**)

68% yield, red, recrystallized from CH_2Cl_2/diethyl ether, m.p. 246–247 °C. Molar conductivity (Ω^{-1} cm^2 mol^{-1}) 84.3. IR (KBr) cm^{-1}: υ (N≡C) 2215. ^{1}H NMR (CD_2Cl_2): δ 4.84 (s, 5H, η^5-C_5H_5), 6.55 (d, 1H, H3, $^3J_{HH}$ = 4.2), 6.98 (d, 1H, H4, $^3J_{HH}$ = 3.9), 7.16 (d, 1H, H11, $^3J_{HH}$ = 4.5), 7.19 (d, 1H, H7, $^3J_{HH}$ = 3.9), 7.32 (d, 1H, H8, $^3J_{HH}$ = 3.9), 7.85 (d, 1H, H12, $^3J_{HH}$ = 4.2); ^{13}C NMR (CD_2Cl_2): δ 82.84 (η^5-C_5H_5), 107.11 (C2), 121.03 (NC), 123.84 (C8), 124.63 (C7), 127.85 (C11), 128.05 (C4), 130.23 (C12), 136.59 (C9), 136.80 (C6), 139.96 (C3), 143.84 (C10), 144.36 (C5), 150.27 (C13); ^{31}P NMR (CD_2Cl_2): δ 79.8. Anal. Calc. for $C_{44}H_{35}F_6N_2O_2P_3S_3Ru$: C, 51.41; H, 3.43, N, 2.72; S, 9.36. Found: C, 51.58; H, 3.36, N, 2.67; S, 9.19%.

4.2.4. RuCp((+)-diop)(NC{SC_4H_2}NO_2)]PF_6 (**1b**)

56% yield, orange-reddish, recrystallized from CH_2Cl_2/*n*-hexane, m.p. 162 °C (dec.). Molar conductivity (Ω^{-1} cm^2 mol^{-1}) 88.5. IR (KBr) cm^{-1}: υ (N≡C) 2205. ^{1}H NMR ($CDCl_3$): δ 4.52 (s, 5H, η^5-C_5H_5), 7.42 (d, 1H, H3, $^3J_{HH}$ = 4.2), 7.80 (d, 1H, H4, $^3J_{HH}$ = 4.2); ^{13}C NMR ($CDCl_3$): δ 84.73 (η^5-C_5H_5), 113.78 (C2), 121.24 (NC), 128.51 (C4), 139.61 (C3), 155.02 (C5); ^{31}P NMR ($CDCl_3$): δ 35.5 (2d, JP_AP_B = 38.1). Anal. Calc. for $C_{41}H_{39}F_6N_2O_4P_3SRu$: C, 51.09; H, 4.08, N, 2.91; S, 3.33. Found: C, 50.95; H, 4.36, N, 2.86; S, 3.02%.

4.2.5. RuCp((+)-diop)(NC{SC_4H_2}$_2NO_2$)]PF_6 (**2b**)

48% yield, orange-reddish, recrystallized from CH_2Cl_2/diethyl ether, m.p. 205–206 °C. Molar conductivity (Ω^{-1} cm^2 mol^{-1}) 86.2. IR (KBr) cm^{-1}: υ (N≡C) 2210. ^{1}H NMR ($CDCl_3$): δ 4.48 (s, 5H, η^5-C_5H_5), 7.20 (d, 1H, H7, $^3J_{HH}$ = 4.2), 7.32 (d, 1H, H4, $^3J_{HH}$ = 3.6), 7.59 (d, 1H, H3, $^3J_{HH}$ = 3.6), 7.86 (d, 1H, H8, $^3J_{HH}$ = 4.2); ^{13}C NMR ($CDCl_3$): δ 84.18 (η^5-C_5H_5), 108.91 (C2), 122.80 (NC), 125.38 (C7), 126.97 (C4), 128.70 (C8), 140.97 (C3), 141.27 (C6), 141.93 (C5), 151.41 (C9); ^{31}P NMR ($CDCl_3$): δ 35.8 (2d, JP_AP_B = 38.1). Anal. Calc. for $C_{45}H_{41}F_6N_2O_4P_3S_2Ru$: C, 51.68; H, 3.95, N, 2.68; S, 6.13. Found: C, 51.82; H, 4.12, N, 2.59; S, 5.98%.

4.2.6. RuCp((+)-diop)(NC{SC_4H_2}$_3NO_2$)]PF_6 (**3b**)

40% yield, red, recrystallized from CH_2Cl_2/diethyl ether, m.p. 145 °C (dec.). Molar conductivity (Ω^{-1} cm^2 mol^{-1}) 81.9. IR (KBr) cm^{-1}: υ (N≡C) 2215. ^{1}H NMR (CD_2Cl_2): δ 4.41 (s, 5H, η^5-C_5H_5), 7.17 (d, 1H, H11, $^3J_{HH}$ = 4.5), 7.20 (d, 1H, H4, $^3J_{HH}$ = 4.5), 7.26 (d, 1H, H7, $^3J_{HH}$ = 4.2), 7.27 (d, 1H, H3, $^3J_{HH}$ = 3.9), 7.35 (d, 1H, H8, $^3J_{HH}$ = 3.9), 7.87 (d, 1H, H12, $^3J_{HH}$ = 4.5); ^{13}C NMR (CD_2Cl_2): δ 84.20 (η^5-C_5H_5), 106.77 (C2), 123.96 (C8), 124.87 (NC), 125.27 (C7), 128.18 (C11), 128.13 (C4), 130.46 (C12), 136.50 (C9), 137.00 (C6), 140.58 (C3), 143.80 (C10), 145.32 (C5), 150.49 (C13); ^{31}P NMR (CD_2Cl_2): δ 36.0 (2d, JP_AP_B = 38.1). Anal. Calc. for $C_{49}H_{43}F_6N_2O_4P_3S_3Ru$: C, 52.17; H, 3.84, N, 2.48; S, 8.53. Found: C, 52.29; H, 3.92, N, 2.39; S, 8.37%.

4.3. Electrochemical studies

The electrochemistry instrumentation consisted of a EG&A Princeton Applied Research Model 273A Potentiometer and experiments were monitored in a PC computer loaded with Model 270 Electrochemical Analysis Software 3.00 of EG&A from Princeton Applied Research. Potentials were referred to a calomel electrode containing a saturated solution of potassium chloride. The working electrode was a 2-mm piece of platinum wire for voltammetry. The secondary electrode was a platinum wire coil. Cyclic voltammetry experiments were performed at room temperature and −20 °C in a PAR polarographic cell. Solutions studied were 1 mM in solute and 0.1 M in tetrabutylammonium hexafluorophosphate as supporting electrolyte. The electrochemical system was checked with a 1 mM solution of ferrocene in acetonitrile and dichloromethane for which the ferrocinium/ferrocene electrochemical parameters ($E_{p/2}$ = 0.38 V in acetonitrile and $E_{p/2}$ = 0.41 V in dichloromethane; ΔE = 60–70 mV; I_a/I_c = 1) were in good agreement with the literature [33,34]. The electrolyte was purchased from Aldrich Chemical Co., recrystallized from ethanol, washed with diethyl ether, and

dried under vacuum at 110 °C for 24 h. Reagent grade acetonitrile and dichloromethane, were dried over P_2O_5 and CaH_2, respectively, and distilled before use under argon atmosphere. An argon atmosphere was maintained over the solution during the experiments.

4.4. Crystal structure determination of the complex **2a**

X-ray data were collected on a MACH3 Enraf–Nonius diffractometer using graphite-monochromated Mo Kα radiation (λ = 0.71073 Å), at room temperature. As a general procedure, the intensity of three standard reflections was measured periodically every 2 h. This procedure did not reveal any appreciable decay. Using the CAD4 software, intensity data were corrected for Lorentz and polarization effects. The position of the Ru atom was obtained by a tridimensional Patterson synthesis, while all the other non-hydrogen atoms were located in subsequent difference Fourier maps. All non-hydrogen atoms were refined by full-matrix least-squares on F^2 with anisotropic thermal motion parameters whereas H-atoms were placed in idealised positions and allowed to refine isotropically riding on the parent C atom. The structure was solved by direct methods with SIR97 [35] and refined by full-matrix least-squares on F^2 with SHELXL97 [36] both included in the package of programs WINGX-VERSION 1.70.01 [37]. Graphical representations were prepared using ORTEP3 [38] and Mercury 1.1.2 [39]. A summary of the crystal data, structure solution and refinement parameters are given in Table 10. Lists of observed and calculated structure factors, tables of final atomic coordinates, anisotropic thermal parameters for all non-hydrogen atoms, hydrogen atomic coordinates, bond lengths and angles, and inter- and intramolecular contact distances are available from the authors and have been deposited as Supplementary material.

4.5. Kurtz powder SHG measurements

The efficiency on Second Harmonic Generation of compounds [RuCp((+)-diop)(NC{SC_4H_2}$_n$$NO_2$)][$PF_6$] **1b**, **2b** and **3b** and [FeCp((+)-diop)(NC{SC_4H_2}$_2$$NO_2$)][$PF_6$] was measured in our laboratories using the Kurtz powder method [27]. The measurements were performed at the fundamental wavelength of 1064 nm originated directly by a Nd:YAG laser at low power (50 mJ per pulse), producing 40 ns pulses with a repetition rate of 10 Hz. The voltage from the photomultiplier was measured by the oscilloscope, which is triggered by the signal itself. The photomultiplier voltage and the neutral density filter area were optimized to obtain a good signal to noise relation and prevent the saturation of the photomultiplier. The oscilloscope measured the time integral of the photomultiplier voltage automatically, which is proportional to the SHG efficiency. The oscilloscope also performed, automatically, the average over several laser shots. The SHG efficiency measurement of the urea reference sample was performed under the same experimental conditions as those of each test sample. For details of our experimental set-up see reference [26].

The procedure for the measurements is as follows: the materials were mulled to a fine powder and compacted in a mount and then installed in the sample holder. Samples grain sizes were not standardized. For this reason, signals between individual measurements were seen to vary in some cases by as much as ±20%. For a proper comparison with the urea reference material the measurements were averaged over several laser thermal cycles.

Table 10
Data collection and structure refinement parameters for **2a**.

Compound	**2a**
Chemical formula	$C_{40}H_{33}F_6N_2O_2P_3RuS_2$
Molecular weight	945.85
Temperature (K)	293(2)
Wavelength (Å)	0.71069
Crystal system	Monoclinic
Space group	$P2_1/n$
a (Å)	13.0721(10)
b (Å)	20.2434(1)
c (Å)	15.6906(1)
α (°)	90.0
β (°)	101.349(1)
γ (°)	90.0
V (Å^3)	4070.9(5)
Z	4
D_c (g cm^{-3})	1.543
Absorption coefficient (mm^{-1})	0.591
F(0 0 0)	1912
Theta range for data collection (°)	1.66–24.97
Limiting indices	$-15 \leqslant h \leqslant 15$; $0 \leqslant k \leqslant 24$; $0 \leqslant l \leqslant 18$
Reflections collected/unique [$R_{(int)}$]	7436/7160 [0.0252]
Refinement method	Full-matrix least-squares on F^2
Data/restraints/parameters	7160/0/538
Goodness-of-fit (GOF) on F^2	1.100
Final R indices [$I > 2\sigma(I)$]	R_1 = 0.0518; wR_2 = 0.0947
R indices (all data)	R_1 = 0.0928; wR_2 = 0.1171
Largest difference peak and hole (e Å^{-3})	0.658 and −0.424

Appendix A. Supplementary material

CCDC 718609 contains the supplementary crystallographic data for **2a**. These data can be obtained free of charge from The Cambridge Crystallographic Data Centre via www.ccdc.cam.ac.uk/data_request/cif. Supplementary data associated with this article can be found, in the online version, at doi:10.1016/j.jorganchem.2009.04.025.

References

[1] D.J. Williams, Angew. Chem., Int. Ed. Engl. 23 (1984) 690.
[2] H.S. Nalwa, Appl. Organomet. Chem. 5 (1991) 349.
[3] N.J. Long, Angew. Chem., Int. Ed. Engl. 34 (1995) 21.
[4] S.R. Marder, in: D.W. Bruce, D. O'Hare (Eds.), Inorganic Materials, 2nd ed., Wiley, Chichester, 1996, p. 121.
[5] T. Verbiest, S. Houbrechts, M. Kauranen, K. Clays, A. Persoons, J. Mater. Chem. 7 (1997) 2175.
[6] I.R. Whittall, A.M. McDonagh, M.G. Humphrey, M. Samoc, Adv. Organomet. Chem. 42 (1998) 291.
[7] E. Goovaerts, W.E. Wenseleers, M.H. Garcia, G.H. Cross, in: H.S. Nalwa (Ed.), Handbook of Advanced Electronic and Photonic Materials, vol. 9, 2001, p. 127 (Chapter 3).
[8] S. Di Bella, Chem. Soc. Rev. 30 (2001) 355.
[9] C.E. Powell, M.G. Humphrey, Coord. Chem. Rev. 248 (2004) 725.
[10] E. Cariati, M. Pizzotti, D. Roberto, F. Tessore, R. Ugo, Coord. Chem. Rev. 250 (2006) 1210.
[11] J.P. Morral, G.T. Dalton, M.G. Humphrey, M. Samoc, Adv. Organomet. Chem. 55 (2008) 61.
[12] M.H. Garcia, A.R. Dias, M. Paula Robalo, M.G. Humphrey, A.M. Mc Donagh, S. Urst, E. Goovaerts, W. Wenseleers, Organometallics 21 (2002) 2107.
[13] E. Goovaerts, W. Wenseleers, P. Hepp, M.H. Garcia, M.P. Robalo, A.R. Dias, M.F.M. Piedade, M.T. Duarte, Chem. Phys. Lett. 367 (2003) 390.
[14] M.H. Garcia, Paulo J. Mendes, A. Romão Dias, J. Organomet. Chem. 690 (2005) 4063.
[15] M.P. Robalo, A. Teixeira, M.H. Garcia, M.F.M. Piedade, M.T. Duarte, A.R. Dias, J. Campo, W. Wenseleers, E. Goovaerts, Eur. J. Inorg. Chem. (2006) 2175.
[16] M.H. Garcia, P.J. Mendes, M.P. Robalo, A.R. Dias, J. Campo, W. Wenseleers, E. Goovaerts, J. Organomet. Chem. 692 (2007) 3027.
[17] W.J. Geary, Coord. Chem. Rev. 7 (1977) 81.
[18] M.H. Garcia, Pedro Florindo, M. Fátima, M. Piedade, M. Teresa Duarte, M. Paula Robalo, Etienne Goovaerts, Wim Wenseleers, J. Organomet. Chem. 694 (2009) 433.
[19] W. Wenseleers, A.W. Gerbrandij, E. Goovaerts, M.H. Garcia, M. Paula Robalo, Paulo J. Mendes, João C. Rodrigues, A.R. Dias, J. Mater. Chem. 8 (1998) 925.
[20] J.L. Oudar, D.S. Chemla, J. Chem. Phys. 66 (1977) 2664.
[21] M.H. Garcia, M.P. Robalo, A.R. Dias, M.F.M. Piedade, A. Galvão, M.T. Duarte, W. Wenseleers, E. Goovaerts, J. Organomet. Chem. 619 (2001) 252.
[22] João C. Rodrigues, Síntese de Novos Materiais Organometálicos com Propriedades de Não Linearidade Óptica, Ph.D. thesis, Faculdade de Ciências da Universidade de Lisboa, 1999.
[23] (a) M.I. Bruce, C. Ean, D.N. Duffy, M.G. Humphrey, G.A. Koutsantonis, J. Organomet. Chem. 295 (1985) C40;
(b) M.I. Bruce, P.A. Humphrey, M.R. Snowe, E.R.T. Tiekink, J. Organomet. Chem. 303 (1986) 417;

(c) M.I. Bruce, A. Catlow, M.G. Humphrey, G.A. Koutsantonis, M.R. Snow, E.R.T. Tiekink, J. Organomet. Chem. 388 (1988) 59;
(d) W.A. Schenk, T. Stur, E. Dombrowski, Inorg. Chem. 31 (1992) 723;
(e) W.H. Pearson, J.E. Shade, J.E. Brown, E. Bitterwolf, Acta Crystallogr. C (1996) 1106.
[24] (a) J.C. Daran, Y. Jeannin, C. Rigault, Acta Crystallogr. C 40 (1984) 249;
(b) J.F. Costello, S.G. Davies, R.M. Highcock, M.E.C. Polywka, M.W. Poulter, T. Richardson, G.G. Roberts, J. Chem. Soc., Dalton Trans. (1997) 105.
[25] C.M. Duff, G.A. Heath, A.C. Willist, Acta Crystallogr. C 46 (1990) 2320.
[26] M.H. Garcia, J.C. Rodrigues, A. Romão Dias, M.F.M. Piedade, M.T. Duarte, M.P. Robalo, N. Lopes, J. Organomet. Chem. 632 (2001) 133.
[27] S.K. Kurtz, T.T. Perry, J. Appl. Phys. 39 (1968) 3798.
[28] J. Ziss, J.L. Oudar, Phys. Rev. A 26 (1982) 2016.
[29] J. Ziss, J.L. Oudar, Phys. Rev. A 26 (1982) 2028.
[30] Ziss, J.F. Nicoud, M. Coquillay, J. Chem. Phys. 81 (1984) 4160.
[31] D.D. Perrin, W.L.F. Amarego, D.R. Perrin, Purification of Laboratory Chemicals, 2nd ed., Pergamon, New York, 1980.
[32] G.S. Ashby, M.I. Bruce, I.B. Tomkins, R.C. Wallis, Aust. J. Chem. 32 (1979) 1003.
[33] I.V. Nelson, R.T. Iwamoto, Anal. Chem. 35 (1961) 867.
[34] R.R. Gagné, Carl A. Koval, G.C. Lisensky, Inorg. Chem. 19 (1980) 2855.
[35] A. Altomare, M.C. Burla, M. Camalli, G. Cascarano, G. Giacovazzo, A. Guagliardi, A.G.G. Moliterini, G. Polidoro, R. Spagna, J. Appl. Cryst. 32 (1999) 115.
[36] G.M. Sheldrick, SHELXL-97: Program for the Refinement of Crystal Structure, University of Gottingen, Germany, 1997.
[37] L.J. Farrugia, J. Appl. Cryst. 32 (1999) 837.
[38] L.J. Farrugia, J. Appl. Cryst. 30 (1997) 565.
[39] C.F. Macrae, P.R. Edgington, P. McCabe, E. Pidcock, G.P. Shields, R. Taylor, M. Towler, J. Van de Streek, J. Appl. Cryst. 39 (2006) 453.